A Comparative Analysis on Process Dependent Structural and Optical Properties of Si-Rich Silicon Carbide Thin Films

Sam Baskar, R. Pratibha Nalini, Gargi Raina

Abstract*: Si nanoclusters (Si-nc) embedded in Silicon Carbide (SiC) matrix are promising for optoelectronic applications. Despite high temperature post fabrication treatments, it is often noticed that the formation of SiC-nc and amorphous-Si nanoclusters (a-Si nc) are favoured than Si nanocrystals. This paper carries out meticulous investigation on the variations in structural and optical properties of amorphous-Silicon rich Silicon carbide (a-Si_xC_y) thin films with varying process conditions in deposition approach, deposition temperatures (T_d) and post deposition annealing conditions. The films deposited by magnetron sputtering and co-sputtering techniques are subjected to various annealing temperatures (T_a) using conventional thermal annealing (CTA), rapid thermal annealing (RTA), vacuum annealing (VA) and in-situ (IA) annealing techniques. A comparative study with deposition and post-deposition conditions considering the effect of excess Si incorporation and the unintentional oxidation during various stages of sample preparation is reported. It is noticed that though Si- nc formed are predominantly amorphous, the films deposited at Td of 200°C and in-situ annealed are promising as they show a higher absorption coefficient (α) and refractive index in comparison with the other high temperature annealing approaches. Such a result paves way to analyse the possibility of these films for future optoelectronic applications at reduced thermal budget.

***Index Terms*: Annealing, Si-rich Silicon carbide, Sputtering, Thin films, Nanoclusters**

I. INTRODUCTION

Alloys based on SiC have always been a material of choice due to their superior mechanical properties and often considered for high-temperature and high-power electronic devices applications [1-3]. Recently, amorphous-Silicon rich Silicon carbide (a-Si_xC_y) and Silicon oxycarbide ($Si_xC_yO_z$) thin films with tailorable compositions are being extensively explored in electronic and MEMS industry, protective coatings, thin film transistors, alternative passivation layer for Si solar cells, gas sensors, electrode materials and in bio-medical applications [4-11]. These films embedded with Si nanocrystals become a preferred optoelectronic material due to the possibility of size dependent band gap engineering [12-15]. However, despite high temperature annealing treatments the phase transformation results in a-Si nc and SiC nc in addition to Si-nc and obtaining high Si-nc density is a challenge.Chemical Vapor Deposition (CVD) as well as Physical Vapor Deposition (PVD techniques have been explored to prepare a-Si_xC_y films [16-23] and it is noted that the radio frequency (R.F) sputtering technique is widely preferred to produce high quality thin films. The variants in the sputtering processes include: sputtering of a SiC target, Co-sputtering of Si and Carbon based targets, reactive sputtering or co-sputtering in the presence of reactive gases to get the desired composition ratio of the film etc.,. [23]. Though a lot of research has been done on the structural and optical properties of a-Si_xC_y films [24-27], the influence on unintentional oxidation during post deposition treatments and their effect on the structural as well as optical properties are barely reported. In this regard, this paper carries out a detailed investigation on the variations in structural and optical properties of amorphous-Silicon rich Silicon carbide (a-Si_xC_y) thin films with varying process conditions in deposition approach, deposition temperatures (T_d) and post deposition annealing conditions. The films deposited by magnetron sputtering and co-sputtering techniques are subjected to various annealing temperatures (T_a) using conventional thermal annealing (CTA), rapid thermal annealing (RTA), vacuum annealing (VA) and *in-situ* (IA) annealing techniques. A comparative study with deposition and post-deposition conditions considering the effect of excess Si incorporation and the unintentional oxidation during various stages of sample preparation is reported.

II. MATERIALS AND METHODS

A. *Thin film deposition*

The a-Si_xC_y films are deposited on a p-type 250-µm Si (100) wafer using RF magnetron sputtering (AJA Orion 5UHV) in the presence of Argon plasma at T_d of 200°C, 350 °C and 500°C. The base pressure and working pressure are 8.0×10^{-7} Torr and 2.0×10^{-3} Torr respectively. Three different approaches are used, the first approach is achieved by sputtering SiC target, and the second approach is by co-sputtering SiC and Si targets. Both the targets are 2 inch in diameter. The RF powers at 13.56 MHz, supplied to the targets (SiC and Si) are varied to get the a-Si_xC_y films. In both approaches, power density to SiC target is maintained at 6.7 $w.cm^{-2}$, whereas, it is varied as 0.9, and 2.2 $w.cm^{-2}$ for Si target in the approach 2.

Revised Manuscript Received on June 12, 2019.

Sam Baskar , Research Scholar, School of Electronics Engineering, VIT University, Chennai
R. Pratibha Nalini, (Resigned) Assistant Professor, School of Mechanical and Building Sciences, VIT University, Chennai
Gargi Raina, Professor, School of Electronics Engineering, VIT University, Chennai.

Published By:
Blue Eyes Intelligence Engineering
& Sciences Publication

The samples are referred in C-series (C2485, C2489, C2485, C2487 and C2486). Subsequently, all the films are annealed under N_2 ambience using conventional thermal annealing (CTA) for 30 min at 750°C, 950°C and 1000°C and Rapid Thermal Annealing (RTA) at 1000°C for 1 min. In the third approach, the Silicon (Si) and Carbon (C) targets are co-sputtered at 200 °C, followed by *in-situ* annealing at 500°C for 30 min. The base pressure, working pressure and the Ar flow is maintained at 1.5x 10^{-7} torr, 3 mtorr and 5 sccm respectively. The input power (density) applied to the Si target is maintained at 4.9 w.cm^{-2} and C target is varied as 2.7, 2.2, and 1.6 w.cm^{-2} respectively for H262, H264 and H266.

B. *Film characterization*

The refractive indices ($n_{1.95eV}$) of the films are investigated by spectroscopic ellipsometry using a HORIBA Jobin-Yvon ellipsometer (UVISEL). The structural properties of the layers are investigated by means of a Thermo Nicolet (Nexus model 670) Fourier transform infrared (FTIR) spectrometer, the analysis between 600-1300 cm^{-1} wavenumber is presented. The chemical composition is analyzed by X-ray photoelectron spectroscopy (Omicron nanotechnology), with a monochromatic Al Ka (1486.5 eV). The band gap of the films is investigated by using FL3-221 series of HORIBA Jobin-Yvon photoluminescence spectroscopy. The excitation wavelength is fixed at 375 nm and the emission spectra are recorded between 200-800 nm.

III. RESULTS AND DISCUSSION

A. *Spectroscopic Ellipsometry (SE)*

The spectroscopic ellipsometry (SE) is a model based non destructive approach to determine thickness and optical constants of thin films. Thicknesses of the films obtained using all the approaches are in the range of 105 nm to 135 nm, and the refractive index ($n_{1.95eV)}$ varies between1.4 -3.9.

Refractive index

In approach 1 (i.e. SiC sputtering at 6.7 w.cm^{-2}), the $n_{1.95eV}$ of as-grown samples varies from 1.48 to 1.85 which upon 1000°C of CTA annealing increased to 1.68 to 2.0. The variation in $n_{1.95eV}$ with increasing T_d may be correlated with the relatively higher packing density and Si incorporation in the films. The ideal values of SiC ranges from 2.5-2.6 (based on the different polytypes, between 1.6 -1.8 for silicon oxycarbide (SiOC) [28], and between 1.45-1.5 for both carbon and SiO_2 [29-30]. Therefore, from the $n_{1.95eV}$ values the film can be assigned to either porous silicon carbide or silicon oxycarbide. In approach 2 (i.e. co-sputtering of SiC and Si), all the set of samples deposited with the power density of 0.9 w.cm^{-2} and 2.2 w.cm^{-2} applied to Si target, show an increasing trend of $n_{1.95eV}$ at all the T_d. The $n_{1.95eV}$ value of approach 2 samples varies between 1.6 to 3.6 suggesting the transition from carbon rich silicon carbide or silicon oxycarbide films to Si-rich silicon carbide upon increasing T_d and T_a. The presence of Si richness is evident and the results are in agreement with values ($n_{1.95eV}$ = 2.3 SiC to 3.6 for Si-rich Si_xC_y) published by Demichelis *et al.* [31] and Janz *et al.*[32]. The approach 3 (i.e. *in-situ* annealing) results in a-Si_xC_y with $n_{1.95eV}$ value of 3.8, 3.8 and 3.9, the absorption coefficient (α) are 1.08, 2.84, and 1.09 x10^5 cm^{-1} respectively for H262, H264 and H266. As compared to other two approaches, the increase in $n_{1.95eV}$ value is attributed to enhanced Si incorporation in the film. Further annealing at1000 °C in N_2 ambience resulted in reduction of $n_{1.95eV}$ value that can be attributed to the unintended dopant impurity or possible crystallization or compositional changes in the film during annealing [33].

B. *Absorption coefficient*

The absorption co-efficient (α) values are ranging from 3.31x10^4 cm^{-1} to 2.25 x10^5 cm^{-1}, which has a correlation with structural properties and nature of the film. The samples C2485, C2489, C2485, C2487 and C2486 show α in 10^4 cm^{-1} and others show α in 10^5 cm^{-1}. The increase in α value is attributed to enhanced Si incorporation which is evident from FTIR and XPS analysis. As compared to other approaches, the approach 3 (in-situ annealed) show highest value absorption coefficient (2.84 x10^5 cm^{-1}) as shown in Fig 1. Generally, the Si-nc in the range of 3-8 nm diameters offers high absorption co-efficient (>10^5 cm^{-1}), however for diameters below 3 nm Si-nc is amorphous and the absorption coefficient enhances by a factor of four compared with its nanocrystalline counterpart [34-35].

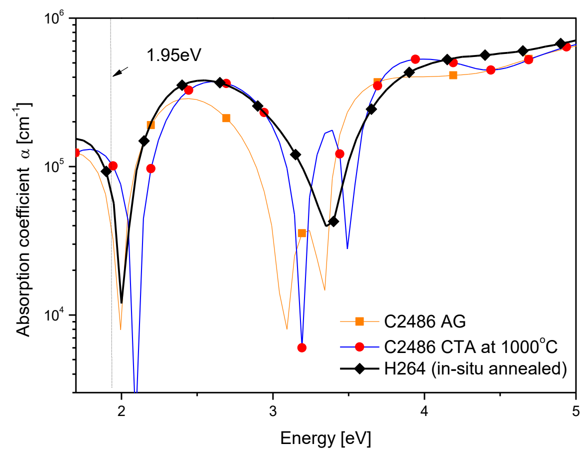

Figure1. Absorption coefficients extracted from SE measurements

C. *Fourier Transform Infrared spectroscopy (FTIR)*

Figure 2 (a) and (b) show the FTIR spectra of as grown samples with absorption coefficient (α) in the range of 10^4 cm^{-1} and 10^5 cm^{-1}. All spectra are broad and have peak centered at 725 cm^{-1}, which is attributed to the stretching vibration of Si-C. The broadness indicates the amorphous nature of the film [30]. It shows a notable change in intensity, shape, with the process parameter. Absence of Si related peaks could be one of the reasons for the reduction in α (10^{4}cm^{-1}). The peaks common amongst these spectra are present at 642-656 cm^{-1}, it can be assigned to Si–O-Si (s) Sym or Si ≡Si related peaks [36, 37]. Upon CTA annealing at 1000°C the peak shifts to 615 cm^{-1} or 635 cm^{-1}, attributed to Si related peaks or Si-O-Si (b) that are present in the sample with α of 10^5 cm^{-1}.

Published By:
Blue Eyes Intelligence Engineering
& Sciences Publication

It is inferred that the presence of Si-O-Si and Si-C band (more of amorphous) also required for enhancing the absorption co-efficient [38]. At T_d of 350ºC, the as grown samples C2485 and C2487 remains more of like a-Si, hence, the α value is similar to of a-Si (~ 2.0 - 4.1x 10^4 cm^{-1}). Upon annealing, there is an enhancement in Si agglomeration as well as Si-C formation. The agglomerated Si interface with Si-C matrix and adsorption of O in Si causes the structure to be in amorphous only. Hence there is increase in α to 10^5 cm^{-1}. The peak around 760 – 740 cm^{-1} indicates the Si-C back bonding with C atom [39]. The α value of Si-C is around ~10^2 cm^{-1}, hence the increased Si-C bonding with improved crystalline nature can reduce the α value. The Si-O-Si can be a possible indication of isolated Si seed or nucleation or an indication of enhanced Si incorporation. In approach 3 (*in-situ* annealed), as the input applied to C target reduces, shift in peak from 610-618 cm^{-1} is observed (in H264), which is attributed Si-Si related bond. The additional peaks and shoulders positioned around 678 cm^{-1}, 817 cm^{-1}, 877 cm^{-1} and 1104 cm^{-1} is attributed to Si-O related bonds [39-42]. This may be due to the bonding of excess Si with oxygen either unintentionally incorporated within the film or the interfacial/surface oxidation. This is in agreement with the models used in SE measurements. Amongst all the approaches, the most optimized samples in terms of $n_{1.95eV}$ and α are considered as a typical sample for further analysis. The C2486 obtained at T_d of 500ºC with SiC 6.7 W/cm^2 and Si 2.2 W/cm^2 from approach 2 and H264 (i.e T_d of 200ºC with Si 4.2 W/cm^2 and C 2.2 W/cm^2) from approach 3 are compared for further analysis.

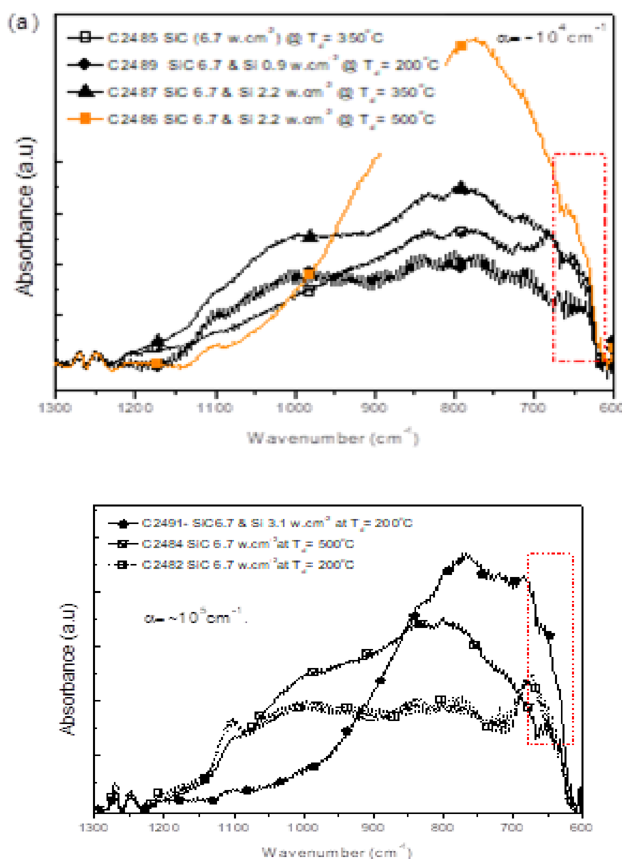

Figure 2 . FTIR spectra of AG samples with absorption coefficient (a) in the range of 10^4 cm^{-1}(b) 10^5 cm^{-1}.

D. ***XPS***

The XPS analysis is carried out on the typical sample from approach 2 (i.e C2486). The XPS spectra of as grown (AG), vacuum annealed (VA) at 1000 ºC and conventional annealed (CTA) at 1350 ºC samples are analyzed to validate the unintentional oxidation and compared with H264 to confirm the Si richness. Figure 3 (a) and (b) show the Si2p and C1s core level of the typical samples respectively. The spectra have peaks of Si 2p, Si 2s, C 1s and O 1s, which confirms the existence of Si, C and O elements in the film surface [43]. In Fig 3 (a), the spectrum of C2486 AG and VA have no trace of Si-O peaks and show a major peak at 99.8 eV, which is attributed to Si–Si ~elemental silicon due to Si agglomeration. The CTA samples has peaks at 102 eV, it is due to intermediate oxidation state of Si which originates from Si in a-Si_xC_y. The peak at 103.2 eV is attributed to Si–O in the Silicon dioxide (SiO_2) [47-48]. However, the H264 (in-situ annealed sample) show no trace of Si-O peaks and has two dominant peak at the binding energy of 99.8 eV and 101 eV, which are attributed to Si–Si and Si–C bonds. These peaks are indicative of an enhancement in Si agglomeration during in-situ annealing, providing an evidence for more Si-nc precipitated in a-Si_xC_y matrix as compared to the as-deposited films at a higher T_d of 500°C. Figure 3 (b) show the carbon related XPS peaking region of the films under study. The spectra of C 1s core level has the following bonds: C–Si (carbon in SiC), C–C (carbon in *a*-C or graphite) and C–O (carbon bonded to O, C–O or C) at 283.2, 284.4, and 286–287 eV binding energies, respectively [44]. On comparing with the spectra of approach 2, it is noticed that the *in-situ* annealed sample has strong Si-Si and Si-C related bonds that confirms the Si richness in a-Si_xC_y film.

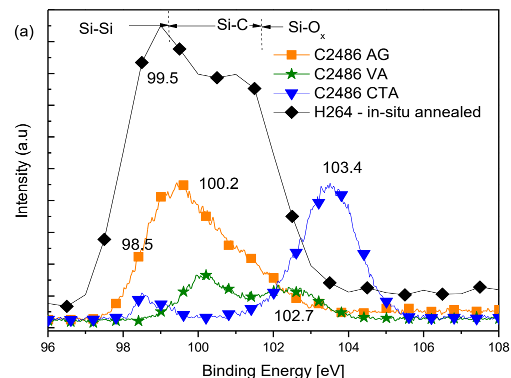

Published By:
Blue Eyes Intelligence Engineering
& Sciences Publication

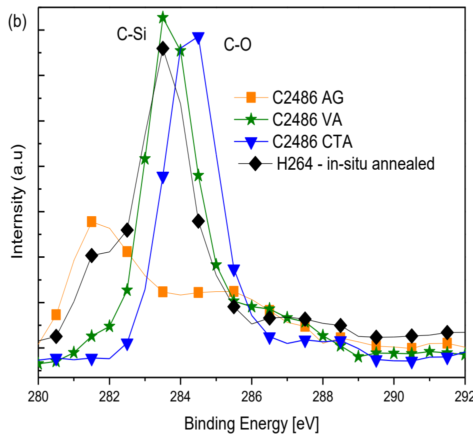

Figure 3 . XPS spectra of optimized samples C2486 and H264 (a) S-2p spectra (b) C-1s spectra

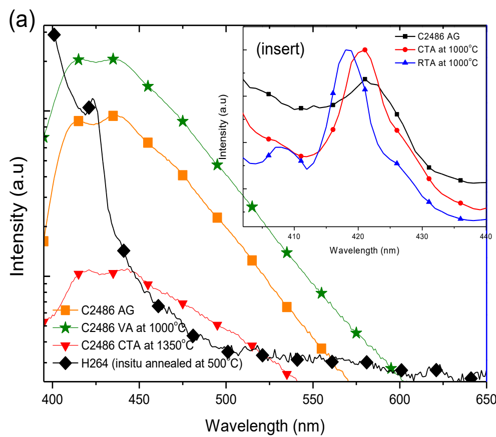

Figure 4 . PL spectra of typical from approach 2 (C2486) and approach 3 (H264)

E. *Photoluminescence spectroscopy*

Figure.4 (a) shows the PL spectra of the typical sample of approach 2 (i.e C2486 AG, VA at 1000 ºC, CTA at 1350 ºC) compared with H264 of approach 3 (in-situ annealed). The inset figure presents the spectra of AG, CTA and RTA annealed at 1000 ºC. The spectra of H264 and C2486 AG has two distinct broad peaks in the blue region, centered at 420, and 436 nm, it is attributed to the quantum confinement or possible nanocluster formation in SiC matrix. The broadness in the spectra indicates the possible presence of multiple luminescent centres [45]. The lower intensity may be attributed to the amorphous nature of the film with unpassivated defects states that provides non-radiative pathways for photoemission. The notable change in spectra between 406 - 430 nm during CTA and RTA has a correlation with the structural and molecular change in the film. There is a reduction in carbon content, increase in Si precipitation and passivation of dangling bands of oxygen upon annealing. At 1000 °C of RTA annealing, the intensity of broader peak at 420 nm increased evolution of sharper peaks centred at 406 nm (equivalent Eg =3.05eV), broader peak at 413 (equivalent Eg = 3.00 eV) and 423 (equivalent Eg = 2.95 eV) nm are noticed. The peak shift (420-423 nm) with the increase of annealing temperature could be due to the quantum confinement or possible nanocluster formation in SiC matrix as reported by Chung et al and J Ma et al. The emergence of peak at 406 nm upon annealing can be attributed to the oxygen related luminescent centers or indication of the possible unintentional oxidation upon annealing [48]In Fig 4 (a), an increase in the intensity and blue shift in the peak positions are noticed upon VA, which could be due to the possible crystallization or surface passivation and the self-aggregation of Si-nc. It is also noticed that, VA shows the highest emission intensity with two prominent peaks centring around 412 nm and 440 nm. These corresponds to an energy gap around 2.9 eV and 2.8 eV respectively. The shifts in the peak position as well as their enhancement in intensity from AG to VA indicate that the emission of the two pronounced peaks are related to luminescent centre from Si-nc and are not defect related. When CTA annealed at 1350oC in Ar, significant reduction in the intensity and red shift in PL peak position are noticed. The quenching of PL could be due to the formation of large Si-nc and a decreasing number of Si-nc caused by the Ostwald ripening phenomena [49]. Using the empirical relation between PL emission peak position (sub band energy) and the Si-nc size reported by,

$$E = 1.56 + 2.4 / D^2$$

where D is the size of the Si-NC; it is noted that there may be Si-NC with different sizes (i.e around 1.2 nm and 1.4 nm) predominantly present contributing to the emission. The stokes shift is evaluated for these two prominent bands as a measure of luminescence energy and absorption energy since the stokes shift is lesser than 1 eV, the nature of Si-nc formed is amorphous [48-50].

IV. CONCLUSION

The a-Si_xC_y films are deposited using RF magnetron sputtering and co-sputtering at different T_d and compositions (Si excess). The effect of various deposition temperatures (T_d), annealing temperatures (T_a), annealing ambiance and film compositions (Si *excess*) on the material properties are investigated using Spectroscopic ellipsometry, FTIR, XPS and PL. From the spectroscopic ellipsometry analysis (the $n_{1.95eV}$ values), it is observed that the increase in T_d and T_a are instrumental for increasing the Si incorporation in the film. The film deposited using approach 1 (i.e. SiC sputtering at 6.7 W/cm^2) appears to be silicon oxycarbide. In approach 2, (i.e. SiC and Si co-sputtering), the $n_{1.95eV}$ value varies between 1.6 to 3.6, suggesting the transition from porous silicon carbide to Si-rich silicon carbide or silicon oxycarbide upon increasing T_d and T_a, which is also supported by the FTIR spectra. The unintentional oxidation is prominent during CTA annealing; it is validated by XPS analysis that supports the reduction in $n_{1.95eV}$ values. The VA at 1000 ºC has enabled more SI-agglomeration in a-Si_xC_y matrix with no-trace of Si-O. However, approach 3, the *in-situ* annealing favor a better reorganization of the phases, avoids contamination and s increasing the quality of Si-rich SiC film ($n_{1.95eV} = 3.88$) with enhanced absorption co-efficient [upto 2.84 x10^5 cm^{-1}]. The possibility of SiC-nc can be reduced and thus the formation of Si-nc can be favored at this lower temperature T_d (i.e 200◦C) and *in-situ* annealing. Improved absorption

co-efficient could be a possible confirmation for the presence of Si-nc in the a-Si_xC_y films. The result obtained in this paper thus suggests a low temperature deposition with in-situ annealing could offer a simple and viable way to tailor the optical constants of the materials. Such a result paves way to analyse the possibility of these films for future optoelectronic applications at reduced thermal budget.

V. ACKNOWLEDGMENT

The authors thank Dr. Fabrice Gourbillea, Research Director of CNS, France, for providing facilities to carryout film deposition and annealing. Dr Mukul Gupta, and Dr. V. Ganesan, Dr. Kiran Singh, at UGC-DAE CSR, Indore, for providing Vacuum annealing facilities. The authors gratefully acknowledge Dr.M.S.Ramachandra Rao, Materials science research center, IIT Madras for providing PL spectroscopic measurement facility.

REFERENCES

1. W.J. Choyke, H. Matsunami and G. Pensl, 'Silicon Carbide: Recent Major Advances', 2nd Edn. Springer, New York, (2003).
2. F. Nava, G. Bertuccio, A. Cavallini and E. Vittones, J.Meas.Sci.Tech.19,102001 (2008).
3. P. M. Sarro, J.Sen and Act 82,210-218 (2000).
4. J. P. Conde, V. Chu, F. Da Silva, A. Kling, Z. Dai, J. C. Soares, S. Arekat, A. Fedorov, M. N. Berberan-Santos F. Giorgis and C. F. Pirri, J. Appl. Phys., Vol. 85, No. 6, (1999).
5. Li Gou, Changsong Qi, Junguo Ran, and Changqiong Zheng, Thin Solid Films 345 42-44(1999).
6. A.K Costa, J.R.Camargo, S.S.Achete and C.A Carius, Thin Solid Films, 243-248 (2000).
7. Rosario Gerhardt, 'Silicon Carbide Based Transit Time Devices', Moumita Mukherjee: 'The New Frontier in High-power THz Electronics, Properties and Applications of Silicon Carbide', in InTech, (2011).
8. J. Huran, A.Valovič, P. Boháček, V.N Shvetsov, A.P. Kobzev, S.B. Borzakov, A. Kleinov, M. Sekáčová, J.Arbet, and V. Sasinková, J.Appl Sur Sci., 269,88-91, (2013).
9. Aylin Karakuscu, Andrea Ponzoni, Parakkulam R. Aravind, Giorgio Sberveglieri, Gian D. Soraru, J. Am. Ceram, 96,2366–2369 (2013).
10. Monika Wilamowska-Zawlocka, Paweł Puczkarski, Zofia Grabowska, Jan Kaspar, Magdalena Graczyk-Zajac, Ralf Riedel and Gian D. Soraru, RSC Adv 6, 104597 (2016).
11. Spyros Gallis, Vasileios Nikas and Alain E. Kaloyeros, 'Modern Technologies for Creating the Thin-film Systems and Coatings':Silicon Oxycarbide Thin films and Nanostructures: Synthesis, Properties and Applications, InTech (2006)
12. J.Y.Fan, X.L.Wu and Paul K. Chu, Progress in Materials Science 51,983-1031(2006).
13. M.A.Ouadfel, A.Keffous, A.Brighet, N.Gabouze, T.Hadjersi, A.Cheriet, M.Kechouane, A. Boukezzata, Y.Boukennous, Y.Belkacem and H.Menari, J.Appl Sur Sci, 265, 94–100,(2013).
14. D.Song, E.C.Cho, Y.H.Cho, G. Conibeer, Y.Huang, S.Huang and M.A.Green, Thin Solid Films 516, 3824–3830 (2008).
15. M. Künle, T.Kaltenbach, P. Löper, A. Hartel, S. Janz, O. Eibl and K.G. Nickel, Thin Solid Films, 519, 151–157(2010).
16. M.Yazdanfar, H.Pedersen, P.Sukkaew, I.G.Ivanov, Ö.Danielsson, O.Kordina, E.Janzén, J.Cry Grow 390, 24–29,(2014).
17. F. Maury, J.M.Agullo, J. Sur and Coat Tech 119-124 (1995).
18. E.Pascual,J.L.Andlijar, E. Fernhndez,E.Bertran J. Dia. Rel.Mat 4,1205-1209, (1995)
19. C.Iliescu and D.P.Poenar, 'Physics and Technology of Silicon Carbide Devices Solution. Chapter 5., PECVD Amorphous Silicon Carbide (α-SiC) Layers for MEMS Applications', InTech, (2013).
20. M. Quadfel, C. Yaddaden, S. Merazga, Cheriet, L.Talb, S.Kaci and H.Menari, J. Alloys and Compounds, 579, 365–37, (2013).
21. N. Ledermann, J. Baborowski, P. Muralt, N. Xantopoulos and J.M. Tellenbach, J.Sur and Coat Tech 125,246–250, (2000).
22. S. Sam Baskar and R. Pratibha Nalini, Materials Today, 3,2121–2131(2016).
23. H. S. Medeiros, R. S. Pessoa, J. C Sagás, M. A. Fraga, L. V. Santos, H. S. Maciel, M. Massi, and A. S. Da Silva Sobrinho, Materials Science Forum,717-720 197-20, (2012).
24. J. López-vidrier, S.Hernández, J. Samà, M.Canino, M. Allegrezza and M. Bellettato, J.Mat Sci & Eng B, 178(9), 639–644(2013).
25. Y.Rui, S. Li, Y.Cao, J. Xu, W.Li and K.Chen,J. App Sur Sci, 269, 37–40,(2013).
26. J.Moon, S.J.Baik, O.Byungsung and J. C. Lee, J. Nanoscale Res Lett,7,503, (2012).
27. R. Gradmann, P.Loeper, M.Künle, M. Rothfelder, S. Janz, M. Hermle, and S.Glunz, Phys. Status Solid C 8, No. 3, 831–834(2011)
28. Yinqiao Peng, Jicheng Zhou, Xuqiang Zheng, Baoxing Zhao and Xiaochao Tan, J. Mod Phy B, Vol. 25, No. 22, 2983–2990 (2011).
29. J. Fan, H. Li, J. Wang and M. Xiao, Appl. Phys. Lett. 101, 131906,6–11,(2012).
30. G. Scardera, T. Puzzer, G. Conibeer, and M. A. Green, J. Appl. Phys., vol.104, 10, (2008).
31. F. Demichelis, Physica B 205,169-174, (1995).
32. S. Janz, S., 'Amorphous Silicon Carbide for Photovoltaic Applications', in KOPS - The Institutional Repository of the University of Konstanz, 1–227, (2006).
33. A. Kole and P. Chaudhuri, Thin Solid Films, vol. 522, 45–49,(2012).
34. P. Löper, D. Hiller, M. Künle, R. Gradmann, S. Janz, M. Hermle, M. Zacharias and S. W. Glunz, Adv. Mater.. 5–7 (2012).
35. S. Kerdiles, A. Berthelot, F. Gourbilleau, R. Rizk, Appl. Phys. Lett., Vol. 76, No. 17, 24,(2000).
36. S. W. King, M. French, J. Bielefeld and W. A. Lanford, J. Non. Cryst. Solids, vol. 357, 2970–2983,(2011).
37. T. Rajagopalan, X. Wang, B. Lahlouh, C. Ramkumar, P. Dutta and S. Gangopadhyay, J.Appl Phy, 94, 5252–5260 (2003).
38. K. Surana, H. Lepage, J. M. Lebrun, B. Doisneau, D. Bellet, L. Vandroux, G. Le Carval, M. Baudrit, P. Thony and P. Mur, Nanotechnology, vol. 23, 10, 105401, (2012).
39. H. S. Medeiros, R. S. Pessoa, J. C. Sagás, M. A. Fraga, L. V. Santos, H. S. Macie, M. Massi and A. S. Da Silva Sobrinhog, Materials Science Forum Vols. 717-720,197-201, (2012).
40. S. Yamada, Y. Kurokawa, S. Miyajima and M. Konagai, Nanoscale Research Letters, 9:246 (2014)
41. Daniel Krcho, 'FTIR Spectroscopy for Silicon Solar Cell'in Characterisation Proceedings of Solar '97 - Australian and New Zealand Solar Energy Society (1997).
42. X. J. Hao, E.-C. Cho, G. Scardera, Y. S. Shen, E. Bellet-Amalric, D. Bellet, G. Conibeer and M. A. Green, Sol. Energy Mater. Sol. Cells, vol. 93, 1524–1530, (2009).
43. Han Liew Juan., 'Structural and electrical characterisations of amorphous silicon carbide films', Mater Theses,. National University of Singapore,(2000).
44. Ling-Hsuan Tsai, Hung-Yu Tai, Chung-Lun Wu, and Gong-Ru Lin, "Enhanced Si Quantum Dot Luminescence in Si- rich SiC Thin-Film Light Emitting Diode" 2012 17thOpto-Electronics and Communications Conference (OECC 2012) Technical Digest July 2012, Busan, Korea
45. Jun Ma, HeBai, Jianjun Zhang, YujieYuan, Jian Ni, Kailiang Zhang, Size-controlled nc-Si:H/a-SiC:H quantum dots superlattice and its application to hydrogenated amorphous silicon solar cells, Solar EnergyMaterials&SolarCells157(2016)923–929
46. C. K. Chung, T. Y. Chen, C. W. Lai, "Low-temperature formation of nanocrystalline SiC particles and composite from three-layer Si/C/Si film for the novel enhanced white photoluminescence", J Nanopart Res (2011) 13:4821–4828
47. Guozhi Wen, Xiangbin Zeng, Xixin Wen, and Wugang Liao, Photoluminescence properties and crystallization of silicon quantum dots in hydrogenated amorphous Si-rich silicon carbide films, Journal of Applied Physics 115, 164303 (2014)
48. Spyros Gallis,Vasileios Nikas, Himani Suhag, Mengbing Huang, Alain E. Kaloyeros, "White light emission from amorphous silicon oxycarbide a-SiCxO thin films: Role of composition and postdeposition annealing, Applied Physics Letters 97, 081905 (2010)
49. Gabriele Brambilla (2017),Testing dissipative magnetosphere model light curves and spectra with fermi pulsars Wavelength-Shifted Yellow Electroluminescence of Si Quantum-Dot Embedded SiNx/SiOx Superlattic by Ostwald Ripening Effect
50. Allan G, Delerue C, Lannoo M.(1996) Physical Review Letters 76: 2961 "Nature of Luminescent Surface States of Semiconductor Nanocrystallites"

Published By:
Blue Eyes Intelligence Engineering
& Sciences Publication
Advanced Technology Engineering and International Journal of
IJEAT
WWW.IJEAT.ORG
Exploring Innovation